

Sub-picosecond acoustic pulses at buried GaP/Si interfaces

Kunie Ishioka,^{1,*} Avinash Rustagi,² Andreas Beyer,³ Wolfgang Stolz,³
Kerstin Volz,³ Ulrich Höfer,³ Hrvoje Petek,⁴ and Christopher J. Stanton²

¹*National Institute for Materials Science, Tsukuba, 305-0047 Japan*

²*Department of Physics, University of Florida, Gainesville, FL 32611 USA*

³*Philipps-University, Material Sciences Center and Faculty of Physics, D-35032 Marburg, Germany*

⁴*Department of Physics and Astronomy, University of Pittsburgh, Pittsburgh, PA 15260, USA*

(Dated: March 11, 2019)

We report on the optical generation and detection of ultrashort acoustic pulses that propagate in three-dimensional semiconductor crystals. Photoexcitation of lattice-matched GaP layers grown on Si(001) gives rise to a sharp spike in transient reflectivity due to the acoustic pulse generated at the GaP/Si interface and detected at the GaP surface and vice versa. The extremely short width of the reflectivity spike, 0.5 ps, would translate to a spatial extent of 3 nm or 10 atomic bilayers, which is comparable with the width of the intermixing layer at the GaP/Si interface. The reflectivity signals are also modified by quasi-periodic Brillouin oscillations of GaP and Si arising from the acoustic pulses during the propagation in the crystals. The present results demonstrate the potential applications of well-defined semiconductor heterointerface as opto-acoustic transducers generating ultrashort acoustic pulses, as well as of the simple optical pump-probe scheme in the nondestructive evaluation of the structural abruptness of buried semiconductor interfaces.

I. INTRODUCTION

Photoexcitation of metals and semiconductors with ultrashort laser pulses can generate strain or shear pulses which propagate into the bulk crystals or along the surfaces [1]. They are induced predominantly through sudden lattice heating (thermoelastic effect) in metals and via deformation potential coupling with (and piezoelectric screening by) photoexcited carriers in semiconductors. These acoustic pulses, widely known as coherent acoustic phonons, have been studied extensively for potential applications in determination of the mechanical properties of solids [2, 3], ultrafast optical control of piezoelectric effect [4] and magnetism [5], development of nanoplasmonic resonators [6] and terahertz polaritons [7].

Coherent acoustic phonons can also be a useful tool in nano-seismology and nano-tomography for characterizing buried interfaces and defective layers, objects hidden under the surfaces, molecules adsorbed on surface and local strains [8–12]. One way to realize ultrashort acoustic pulses for higher spatial resolution in these applications is to generate surface acoustic waves (SAWs) using one- or two-dimensional metallic nano-gratings. The shortest wavelength of SAWs achieved so far was 45 nm, determined by the periodicity of the grating [13]. Another approach is to confine coherent acoustic phonon pulses into sub-micron scale objects. The shortest acoustic pulse actually measured, with a wavelength of 150 nm, was achieved by focusing an acoustic pulse inside a metal-coated silica fiber [14]. However, transferring such short acoustic pulses into a three-dimensional crystal without increasing its wavelength has been a great challenge [15].

Optical generation of acoustic pulses in indirect band gap semiconductors GaP and Si without aid of metallic transducers has been studied recently in pump-probe reflectivity scheme [16]. The generation of the acoustic pulses in these semiconductors originated from the short (~ 100 nm) absorption length of the pump light. GaP can be grown with nearly perfect lattice match on exact Si(001) substrate, and the intermixing layer at the interface can be reduced to $\lesssim 7$ atomic bilayers [17, 18]. The combination of the two semiconductors therefore has the potential not only for Si based opto-electronic devices and high efficiency multi-junction solar cells but also for opto-acoustic transducers.

In the present paper, we report on coherent acoustic phonons generated by excitation of the GaP/Si interface with a femtosecond laser pulse. Transient reflectivity responses exhibit a sharp spike at a time delay corresponding to the travel of the normal strain across the GaP layer, confirming its origin as an acoustic pulse generated at the GaP/Si interface and detected at the GaP surface and vice versa. The spatial extent of the acoustic pulse can be directly estimated from the temporal width of the reflectivity spike. The transient reflectivity responses also exhibit quasi-periodic Brillouin oscillations arising from the acoustic pulses during their propagation in the three-dimensional crystals. Our theoretical modeling supports our interpretation that photoexcited carriers accumulated in the vicinity of the interface and surface give rise to the observed reflectivity changes.

II. EXPERIMENTAL METHODS

The samples studied are nominally undoped GaP films grown by metal organic vapor phase epitaxy on n -type Si(001) substrates with different thicknesses from $d = 16$ to 56 nm. Details of the sample preparation and the

* ishioka.kunie@nims.go.jp

evaluation of the atomic-scale structure are described elsewhere [17]. Transmission electron microscopy (TEM) images confirm that all the GaP layers have smooth surfaces and abrupt GaP/Si interfaces with intermixing of $\lesssim 7$ atomic bilayers [18], while the density of planar defects is minimized. The thicknesses of the GaP layers are measured by x-ray diffraction.

Pump-probe reflectivity measurements are performed in a near back-reflection configuration using laser pulses with 400-nm wavelength (3.1-eV photon energy) and 10-fs duration [19]. Pump-induced change in the reflectivity ΔR is measured as a function of time delay between pump and probe pulses using a fast scan technique. The optical absorption depth, $\alpha_{\text{GaP}}^{-1} = 116$ nm [20], exceeds the GaP film thicknesses ($d=56$ nm at maximum). The 3.1-eV photons are also absorbed strongly by the Si substrate ($\alpha_{\text{Si}}^{-1} = 82$ nm).

III. EXPERIMENTAL RESULTS

Figure 1a compares the reflectivity responses from the GaP films of different thicknesses d on Si, together with those of the bulk GaP and Si already reported in Ref. [16]. All the traces show step rise or drop at $t=0$, followed by recovery on a time scale of 1 ps (Fig. 1b), which arises from the photoexcited carrier dynamics. The reflectivity traces are also modulated by oscillations with sub-100 fs periods and several ps dephasing times due to the generation of coherent optical phonons of GaP and Si, whose details have been reported elsewhere [21].

On the longer time scale, the reflectivity traces of the GaP/Si samples show quasi-periodic oscillations on tens of picoseconds time scale, as shown in Fig. 1a. Similar but more regular oscillations are observed for bulk GaP and Si, and attributed to the interference between the probe beam reflected from the surface and also from the propagating strain pulse [16]. The frequency f_B of such an oscillation, sometimes referred to as Brillouin oscillation, is given by $f_B = 2nv/\lambda = 123$ and 235 GHz for GaP and Si for normal incidence, with n being the refractive index, v , the longitudinal acoustic (LA) phonon velocity, and λ , the probe wavelength [1, 16]. Fourier-transformed (FT) spectra for the thickest ($d=56$ nm) and thinnest ($d=16$ nm) GaP films (Fig. 1c) are dominated by a peak at f_B^{GaP} and a dip at f_B^{Si} , confirming an acoustic pulse propagating in the GaP film and in the Si substrate as the main origin of the reflectivity modulation, respectively. We note that the f_B^{Si} component appears as a dip because of the interference with the large non-oscillatory electronic response in the reflectivity, which we do not subtract before performing the Fourier transform. The FT spectra for the intermediate thicknesses ($d=35$ and 45 nm), by contrast, have both f_B^{GaP} and f_B^{Si} components, indicating that both the acoustic pulses moving in GaP and in Si are contributing.

In addition to the quasi-periodic modulations, the reflectivity traces from the GaP/Si samples exhibit extra

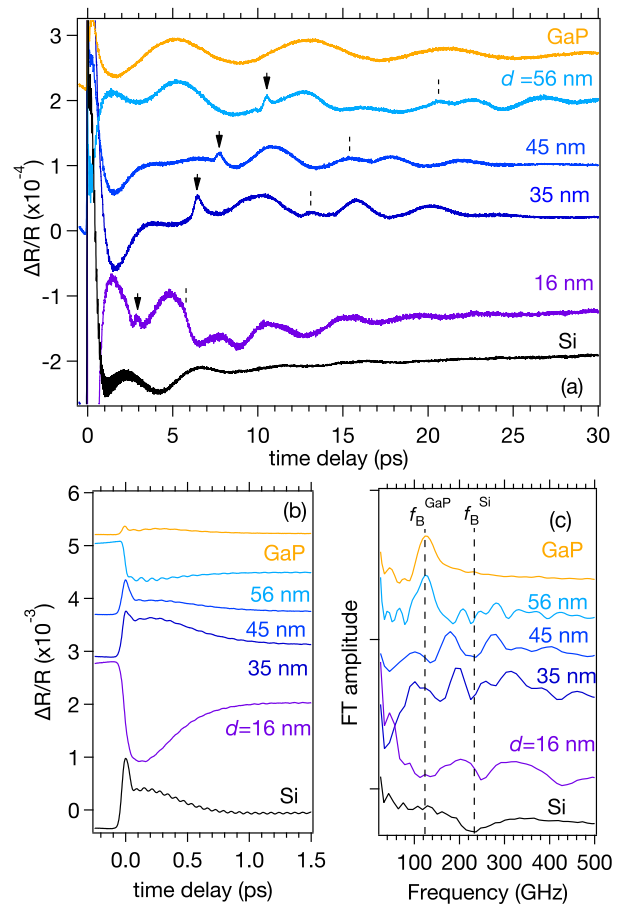


FIG. 1. (Color Online.) (a,b) Reflectivity changes of the GaP films of different thicknesses d on Si(001) substrates, together with those of bulk Si and GaP. Pump densities are $90\mu\text{J}/\text{cm}^2$ for bulk Si and $30\mu\text{J}/\text{cm}^2$ for other samples. (a) and (b) show identical traces with different vertical and horizontal scales. Arrows and broken lines in (a) indicate the first and second reflectivity spikes. (c) Fourier-transformed spectra of the reflectivity changes for time delay $t > 0.1$ ps.

features seen as sharp spikes, as indicated by arrows in Fig. 1a. These spikes are absent for bulk GaP and Si and therefore characteristic of the interface. The most intriguing feature of the spike is its extremely short (~ 0.5 ps) temporal width, as shown in Fig. 2b. The temporal width translates to a spatial extent of ~ 3 nm or ~ 10 atomic Ga-P bilayers, which is comparable with the thickness of the GaP-Si intermixing region at the interface, 7 atomic bilayers [18]. The spikes appear at delay times $t \simeq \tau_0 \equiv d/v^{\text{GaP}}$, as shown in Fig. 2a, with $v^{\text{GaP}} = 5.847$ nm/ps being the group velocity of the LA phonon of GaP in the [001] direction [22]. The appearance times imply that the reflectivity spikes are induced by the LA phonon wave packet after traveling in the GaP film *one way*, i.e., by acoustic pulses generated at the GaP/Si interface and detected at the GaP/air surface, and/or vice versa. We also see smaller and broader spikes in the reflectivity at $t \simeq 2\tau_0$, as indicated by broken lines in Fig. 1a

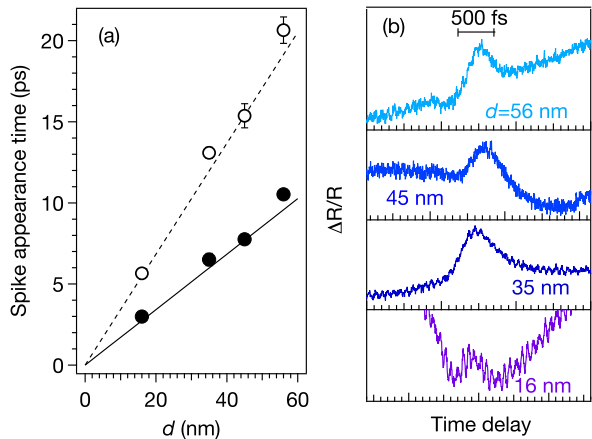


FIG. 2. (Color Online.) (a) Appearance times of the first and second reflectivity spikes (filled and open circles) as a function of the GaP film thickness d . Solid and broken lines represent $t = \tau_0 \equiv d/v^{\text{GaP}}$ and $t = 2\tau_0$. (b) Expanded reflectivity traces showing the first spikes.

and by open symbols in Fig. 2a. These second spikes can correspond to an acoustic pulse generated at the GaP/Si interface or GaP/air surface, and detected after a round trip in the GaP layer.

The possible time evolution of the acoustic pulses generated at the interface and at the surface are schematically shown with solid lines in Fig. 3a, neglecting the small ($\lesssim 0.1$) reflection from the interface. For $0 < t \leq \tau_0 = d/v^{\text{GaP}}$ (temporal regime I) we expect the acoustic pulse generated at the GaP/Si interface to propagate in both directions into the GaP and Si layers, and the pulse generated at the GaP surface to move into the GaP layer. For $\tau_0 < t \leq 2\tau_0$ (regime II) the pulse from the surface enters into the Si, whereas the pulse from the interface is reflected at the GaP surface and propagates back to the interface. For $t > 2\tau_0$ (regime III) all three pulses propagate in the Si layer. Based on these expectations we fit the experiments to the sum of two harmonic oscillations in regimes I and II with fixed frequencies at f_B^{GaP} and f_B^{Si} (neglecting the damping), and to a single damped harmonic oscillation at f_B^{Si} in regime III. The obtained fits, shown with oscillation components in Fig. 3b and compared with the experiments in Fig. 4, can reproduce the experimental $\Delta R/R$ reasonably well for $d \geq 35$ nm, except for the sharp spike at $t = \tau_0$. We see that the oscillation component at f_B^{Si} has distinct discontinuities at both $t = \tau_0$ and $2\tau_0$, confirming that the acoustic pulses are indeed generated both at the surface and at the interface. For the thinnest GaP layer ($d = 16$ nm), however, we cannot determine the oscillation component at f_B^{GaP} in regimes I and II because the fitting time window width τ_0 is too small compared with $1/f_B^{\text{GaP}}$. Moreover, we need to introduce an additional discontinuity at $t \sim 3\tau_0$ to fit the experiment, suggesting that the reflection of the acoustic pulse at the GaP/Si interface is not

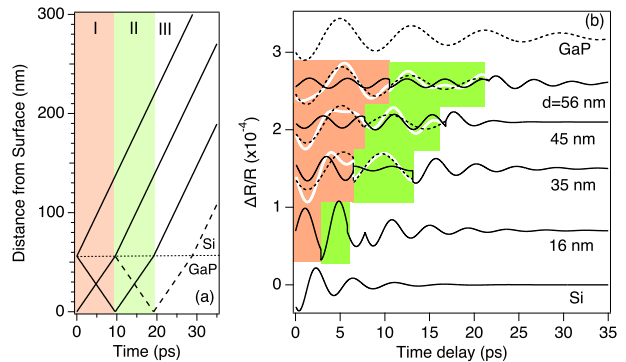


FIG. 3. (Color Online.) (a) Schematic diagram of the acoustic pulse positions as a function of time in the case of $d = 56$ nm. Acoustic pulses are generated at the GaP/Si interface and GaP surface at $t = 0$, and propagate in GaP and Si at v^{GaP} and v^{Si} . Broken line represents the acoustic pulse position taking into account the reflection at the interface. (b) Fits of the experimental Brillouin oscillations to a double damped harmonic function. White solid curves in shaded areas represent the fit results, whereas the black broken and solid curves represent the oscillation components at frequencies f_B^{GaP} and f_B^{Si} . Areas shaded in red and green represent temporal regimes I ($0 < t \leq \tau_0$) and II ($\tau_0 < t \leq 2\tau_0$) in both panels.

negligible for this sample, as indicated with broken lines in Fig. 3a.

IV. THEORETICAL MODELING AND DISCUSSION

We have also theoretically modeled the optical generation and detection of an acoustic pulse at the GaP/Si heterointerface in the similar manner as those for bulk crystals [16]. The details of the modeling are described in the Supplementary Information [23]. We assume that a normal strain η is generated predominantly via the deformation potential interaction with photoexcited carriers, and that the strain induces a change in the dependence of the dielectric constant ϵ on the probe photon energy E . Both the generation and detection processes depend on the relative deformation potential coupling constant, a_{cv} , defined by the difference between the coupling constants of the conduction and valence bands. If we assume the carrier density $N(z)$ at distance from the surface z is proportional to the product of the absorption coefficient $\alpha(z)$ and the pump light intensity $I(z)$, as we did for bulk GaP and Si [16], we obtain N , and thereby the strain η , that decay exponentially with z and have a distinct kink at $z = d$ (case 1 in Fig. S1ab in Supplementary Information [23] and Fig. 4a). This type of strain, however, can reproduce neither the Brillouin oscillation nor the sharp spike of the experimental reflectivity changes, as shown in Fig. S2 in Supplementary Information [23] and as case 1 in Fig. 4b, regardless of the choice of the

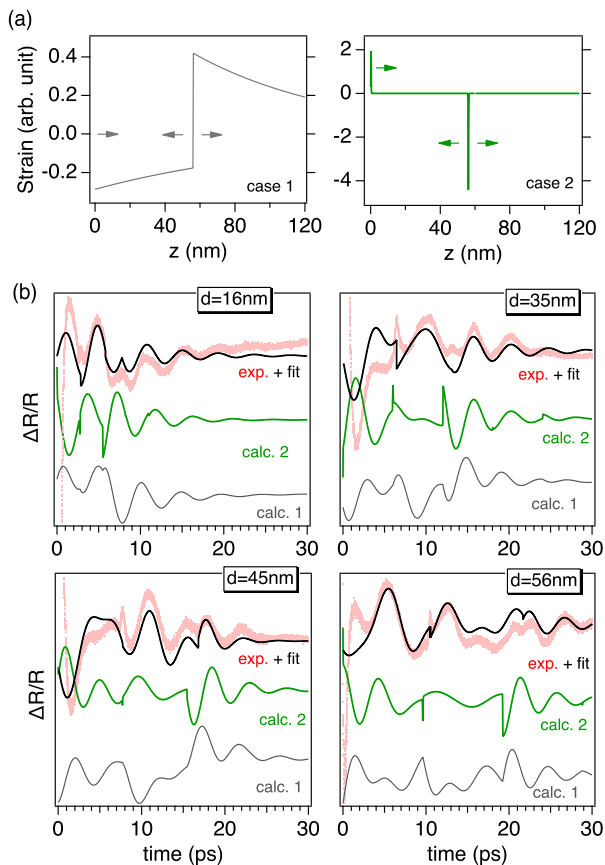


FIG. 4. (Color Online.) (a) (a) Calculated depth profiles of the strain at $t = 0$ for the 56-nm thick GaP layer on Si. Arrows indicate the directions of the strain propagations for $0 < t < \tau_0$. (b) Comparison of calculated reflectivity changes with experimental reflectivity changes and their fit results for GaP/Si samples with different thicknesses. Traces are offset for clarity. The calculations in both (a) and (b) assume *as-excited* carrier distribution under flat electronic bands (case 1) and carriers localized at the interface and the surface under steep band bending (case 2). The relative deformation potential coupling constants $a_{cv}^{\text{GaP}} = 2.25$ eV and $a_{cv}^{\text{Si}} = -4.52$ eV are used for the both cases.

coupling constants a_{cv}^{GaP} and a_{cv}^{Si} .

The failure of the *as-excited* carrier distribution suggests that we need to take into account the redistribution of the photoexcited carriers occurring on shorter time scale than the acoustic pulse generation. Indeed, the efficient generation of the coherent *optical* phonons of GaP, which are observed simultaneously in the transient reflectivity changes (Fig. 1b), indicates ultrafast separation of the photoexcited electrons and holes within ~ 100 fs in the presence of space charge field (Fig. S1c in Supplementary Information [23]) [21]. We model the carrier distribution N after the charge separation with Gaussian functions centered at $z = 0$ and $z = d$ (case 2 in Fig. S1a in Supplementary Information [23]) and calculate the induced strain η and reflectivity change $\Delta R/R$. The calculated reflectivity changes, shown in Fig. S3 in Sup-

plementary Information [23] as well as case 2 in Fig. 4b, reproduce the experimental Brillouin oscillations reasonably well with positive a_{cv}^{GaP} and negative a_{cv}^{Si} . They also feature a distinct spike at $t = \tau_0$, though it appears either as a negative dip or a positive peak depending on d . The calculations support that the photoexcitation predominantly creates ultrashort strain pulses at the GaP/Si interface and the GaP surface, rather than the kinked exponential strain that are similar with those for bulk GaP and Si crystals.

Our calculations, even in case 2, cannot reproduce the experimentally observed reflectivity spike quantitatively for all d , as long as we use a single combination of a_{cv}^{GaP} and a_{cv}^{Si} . The appearance of the calculated spike as a negative dip for some d and as a positive peak for others suggests that the sign of a_{cv} can depend on the GaP layer thickness at the actual interfaces. It also indicates the limit of the present modeling, in which we use the same values of a_{cv}^{GaP} and a_{cv}^{Si} in describing both the generation and the detection. Whereas this was a reasonable approximation for the bulk crystals, in which the generation and the detection occur in the same material [16], for the heterointerfaces the acoustic pulse generated in one material and detected in another can make the reflectivity response more complicated. Our theoretical modeling also includes the effect of ultrafast carrier dynamics in a very limit way. A recent study on a GaAs/transition metal oxide (TMO) interface reported the delayed generation of intense coherent LA phonons only when pumped from the back side of the GaAs film, and attributed it to the photoexcited holes drifted to the front surface due to the steep built-in field and accumulated at the GaAs/TMO interface [24]. We can also expect a similar ultrafast charge dynamics to contribute directly to the acoustic pulse generation at the GaP/Si interfaces. To include such dynamic effects in theoretical modeling, however, is beyond the scope of the present study. The present experimental and theoretical results nevertheless demonstrate the generation of the ultrashort acoustic pulse that has no match in other materials by making use of well-defined semiconductor heterointerface and its optical detection in a simple pump-probe scheme.

V. CONCLUSION

We have demonstrated that excitation of GaP/Si(001) heterointerfaces with femtosecond laser pulses induces ultrashort acoustic pulses, which are directly observed as sharp spikes in the transient reflectivity changes. The sub-picosecond durations of the acoustic pulses are comparable with intermixing layer thickness at the GaP/Si interfaces, and considerably shorter than those reported in the previous studies. The results suggest that the well-defined semiconductor heterointerfaces can be used as opto-acoustic transducers to generate ultrashort acoustic pulses. The direct observation of the acoustic pulse shape in the transient reflectivity enables nondestructive eval-

uation of the structural abruptness of the buried semiconductor heterointerface on nanometer scale in a simple optical pump-probe scheme.

ACKNOWLEDGMENTS

This work is partly supported by the Deutsche Forschungsgemeinschaft through SFB 1083 and HO2295/8, as well as by NSF grant DMR-1311845 (Petek) and DMR-1311849 (Stanton).

-
- [1] C. Thomsen, H. Grahn, H. Maris, and J. Tauc, *Phys. Rev. B* **34**, 4129 (1986).
- [2] H. Ogi, M. Fujii, N. Nakamura, T. Yasui, and M. Hirao, *Phys. Rev. Lett.* **98**, 195503 (2007).
- [3] A. Lomonosov, A. Ayouch, P. Ruello, G. Vaudel, M. Baklanov, P. Verdonck, L. Zhao, and V. Gusev, *ACS Nano* **6**, 1410 (2012).
- [4] C.-K. Sun, Y.-K. Huang, J.-C. Liang, A. Abare, and S. DenBaars, *Appl. Phys. Lett.* **78**, 1201 (2001).
- [5] J.-W. Kim, M. Vomir, and J.-Y. Bigot, *Sci. Rep.* **5**, 8511 (2015).
- [6] K. O'Brien, N. Lanzillotti-Kimura, J. Rho, H. Suchowski, X. Yin, and X. Zhang, *Nat. Commun.* **5**, 4042.
- [7] R. Koehl and K. Nelson, *J. Chem. Phys.* **114**, 1443 (2001).
- [8] O. Wright and K. Kawashima, *Phys. Rev. Lett.* **69**, 1668 (1992).
- [9] G. Tas, J. Loomis, H. Maris, A. Bailes, and L. Seiberling, *Appl. Phys. Lett.* **72**, 2235 (1998).
- [10] M. Hettich, K. Jacob, O. Ristow, C. He, J. Mayer, M. Schubert, V. Gusev, A. Bruchhausen, and T. Dekorsy, *Appl. Phys. Lett.* **101**, 191606 (2012).
- [11] S. Kashiwada, O. Matsuda, J. Baumberg, R. Voti, and O. Wright, *J. Appl. Phys.* **100**, 073506 (2006).
- [12] T. Dehoux, O. Wright, R. Voti, and V. Gusev, *Phys. Rev. B* **80**, 235409 (2009).
- [13] Q. Li, K. Hoogeboom-Pot, D. Nardi, M. Murnane, H. Kapteyn, M. Siemens, E. Anderson, O. Hellwig, E. Dobisz, B. Gurney, R. Yang, and K. Nelson, *Phys. Rev. B* **85**, 195431 (2012).
- [14] T. Dehoux, K. Ishikawa, P. Otsuka, M. Tomoda, O. Matsuda, M. Fujiwara, S. Takeuchi, I. Veres, V. Gusev, and O. Wright, *Light Sci Appl.* **5**, e16082 (2016).
- [15] V. Temnov, C. Klieber, K. Nelson, T. Thomay, V. Knittel, A. Leitenstorfer, D. Makarov, M. Albrecht, and R. Bratschitsch, *Nat Commun* **4**, 1468 (2013).
- [16] K. Ishioka, A. Rustagi, U. Höfer, H. Petek, and C. Stanton, *Phys. Rev. B* **95**, 035205 (2017).
- [17] A. Beyer, J. Ohlmann, S. Liebich, H. Heim, G. Witte, W. Stolz, and K. Volz, *J. Appl. Phys.* **111**, 083534 (2012).
- [18] A. Beyer, A. Stegmüller, J. Oelerich, K. Jandieri, K. Werner, G. Mette, W. Stolz, S. Baranovskii, R. Tönnner, and K. Volz, *Chem. Mater.* **28**, 3265 (2016).
- [19] K. Ishioka, K. Brixius, U. Höfer, C. Stanton, and H. Petek, *Phys. Rev. B* **92**, 205203 (2015).
- [20] D. Aspnes and A. Studna, *Phys. Rev. B* **27**, 985 (1983).
- [21] K. Ishioka, K. Brixius, A. Beyer, A. Rustagi, C. Stanton, W. Stolz, K. Volz, U. Höfer, and H. Petek, *Appl. Phys. Lett.* **108**, 051607 (2016).
- [22] R. Weil and W. Groves, *J. Appl. Phys.* **39**, 4049 (1968).
- [23] <http://www.nims.go.jp/ldynamics/eprints/Supplement1865789.pdf>.
- [24] K. L. Pollock, H. Q. Doan, A. Rustagi, C. J. Stanton, and T. Cuk, *J. Phys. Chem. Lett.* **8**, 922 (2017).